Chinese Journal of
POLYMER SCIENCE 高分子科学

Direct Comparison of Crystal Nucleation Activity of PCL on Patterned Substrates

Hu Jian, Xin Rui, Hou Chun-Yue, Yan Shou-Ke, Liu Ji-Chun

Cite this article as:
Hu Jian, Xin Rui, Hou Chun-Yue, Yan Shou-Ke, Liu Ji-Chun. Direct Comparison of Crystal Nucleation Activity of PCL on Patterned Substrates[J]. *Chinese J. Polym. Sci*, 2019, 37(7): 693-699. doi: 10.1007/s10118-019-2226-z

View online: https://doi.org/10.1007/s10118-019-2226-z

Articles you may be interested in

A REAL-TIME AFM STUDY ON CRYSTAL NUCLEATION AND GROWTH IN NANODROPLETS OF ISOTACTIC POLYPROPYLENE

Chinese J. Polym. Sci. 2013, 31(9): 1310 https://doi.org/10.1007/s10118-013-1330-8

How Polydispersity of Network Polymers Influences Strain-induced Crystal Nucleation in a Rubber

Chinese J. Polym. Sci. 2014, 32(9): 1218 https://doi.org/10.1007/s10118-014-1495-9

Application of Successive Self-nucleation and Annealing to Study the Stereo-defects Distribution of Biaxially Oriented Polypropylene

Chinese J. Polym. Sci. 2014, 32(3): 362 https://doi.org/10.1007/s10118-014-1412-2

聚乙烯树脂的连续自成核与退火热分级实验参数优化及其与逐步结晶热分级对比

Parameters Optimization of Successive Self-nucleation/Annealing Thermal Fractionation Experiments for Polyethylene Resin and Comparison with Step Crystallization

高分子学报. 2015(3): 326 https://doi.org/10.11777/j.issn1000-3304.2015.14281

流场作用对聚丙烯结晶成核过程和晶体生长过程动力学的影响

Influence of Shear Flow on the Crystallization Kinetics of Isotactic Polypropylene in Nucleation and Crystal Growth Processes

高分子学报. 2015(4): 396 https://doi.org/10.11777/j.issn1000-3304.2015.14314

左旋聚乳酸/聚(ε-己内酯)共混物在取向聚乙烯基底上的附生结晶行为

Epitaxy of PLLA/PCL Blends on Highly Oriented Polyethylene Substrate

高分子学报. 2017(9): 1524 https://doi.org/10.11777/j.issn1000-3304.2017.17109

Chinese Journal of
POLYMER SCIENCE

ARTICLE

https://doi.org/10.1007/s10118-019-2226-z
Chinese J. Polym. Sci. **2019**, *37*, 693–699

Direct Comparison of Crystal Nucleation Activity of PCL on Patterned Substrates

Jian Hu[a], Rui Xin[a], Chun-Yue Hou[a], Shou-Ke Yan[a*], and Ji-Chun Liu[b]

[a] *Key Laboratory of Rubber-Plastics, Ministry of Education/Shandong Provincial Key Laboratory of Rubber-plastics, Qingdao University of Science & Technology, Qingdao 266042, China*
[b] *College of Chemical Engineering and Pharmaceutics, Key Laboratory of Polymer Science and Nanotechonology, Henan University of Science and Technology, Luoyang 471003, China*

Abstract A sample containing different regions with poly(ε-caprolactone) (PCL), oriented polyethylene (PE), and oriented isotactic polypropylene (*i*PP) films in contact with glass slide has been prepared to be observed in the same view field in an optical microscope and the crystallization of PCL in different regions during cooling from 80 °C down to room temperature at a rate of 1 °C·min^{-1} was studied. The results showed that the crystallization of PCL started first at the PE surface and then at the *i*PP surface, while its bulk crystallization occured much later. This indicates that though both PE and *i*PP are active in nucleating PCL, the nucleation ability of PE is stronger than that of *i*PP. This was due to a better lattice matching between PCL and PE than that between PCL and *i*PP. Moreover, since lattice matching existed between every (*hk*0) lattice planes of both PCL and PE but only between the $(100)_{PCL}$ and $(010)_{iPP}$ lattice planes, the uniaxial orientation feature of the used PE and *i*PP films resulted in the existence of much more active nucleation sites of PCL on PE than on *i*PP. This led to the fact that the nucleation density of PCL at PE surface was so high that the crystallization of PCL at PE surface took place in a way like the film developing process with PCL microcrystallites happened everywhere with crystallization proceeding simultaneously. On the other hand, even though *i*PP also enhanced the nucleation density of PCL evidently, the crystallization of PCL at *i*PP surface included still a nucleation and crystal growth processes similar to that of its bulk crystallization.

Keywords Poly(ε-caprolactone); Polypropylene; Polyethylene; Epitaxy; Heterogeneous nucleation

Citation: Hu, J.; Xin, R.; Hou, C. Y.; Yan, S. K.; Liu, J. C. Direct comparison of crystal nucleation activity of PCL on patterned substrates. *Chinese J. Polym. Sci.* **2019**, *37*, 693–699.

INTRODUCTION

Heterogeneous nucleation is not only a commonly encountered phenomenon of polymer crystallization, but also fundamentally important for understanding the polymer crystallization, which shows great influence on the morphology and consequently the mechanical property of semicrystalline polymers.[1–6] Therefore, it has been intensively studied for a long time, which leads to a great progress towards a better understanding of it. As a typical heterogeneous nucleation system, surface-induced polymer crystallization has attracted considerable attention in the past several decades. The research in this field concerns mostly the influence of a foreign surface (the substrate) on the crystal modification of a polymer (the overgrowth polymer) as well as its nucleation mechanism and efficiency. The nucleation efficiency is frequently characterized by comparing the nucleation density of the polymer in bulk or at the surface of a substrate through optical microscopy observation equipped with a hot stage. As an example, for the fiber reinforced polymer composite systems,[7–9] through counting the nucleus number of a polymer formed at fiber surface, the fibers have been classified into three categories with respect to their nucleation efficiency, *i.e.*, active, moderate, and inactive ones. It should be pointed out that this method gives only a qualitative description of the heterogeneous nucleation behavior at relatively low supercooling, since the counting of nucleus number is hardly achieved at high supercoolings. Therefore, a quantitative way for characterizing the nucleation efficiency was established in 1993.[10,11] It is measured by the quantity $100 \times (T_{ca} - T_{c1})/(T_{c2} - T_{c1})$ expressed in form of percentage. Here, T_{c1} and T_{ca} are the peak crystallization temperatures of the polymer in bulk and at the substrate surface in the cooling process at a rate of 10 °C·min^{-1}, respectively. T_{c2} is the optimal self-nucleating crystallization temperature and determined by first heating the neat polymer up to a temperature *ca*. 20 °C above its equilibrium melting point for erasing previous thermal history and cooling down to room temperature for a complete crystallization. The sample was subsequently heated up to the desired temperature and cooled down at a rate of 10 °C·min^{-1}. The highest peak crystallization temperature in the second cooling process is then used as T_{c2}.

It should be noted here that in the aforementioned ways for comparing the nucleation efficiency, either qualitatively

* Corresponding author: E-mail skyan@qust.edu.cn

Received December 24, 2018; Accepted January 17, 2019; Published online February 27, 2019

© Chinese Chemical Society
Institute of Chemistry, Chinese Academy of Sciences
Springer-Verlag GmbH Germany, part of Springer Nature 2019

or quantitatively, separate experiments are needed for different crystallization processes. In this way, changes in experimental parameters, such as sample thickness, molten status of the polymer, temperature *etc.*, may be expected. This will unambiguously influence the obtained results. Taking this into account, if a sample contains different regions with a polymer in contact to varied substrates in the same view field, as illustrated in Fig. 1, then the polymer in different regions will be crystallized under exactly the same conditions. Consequently, the above-mentioned uncertainty in the experimental procedure can be avoided.

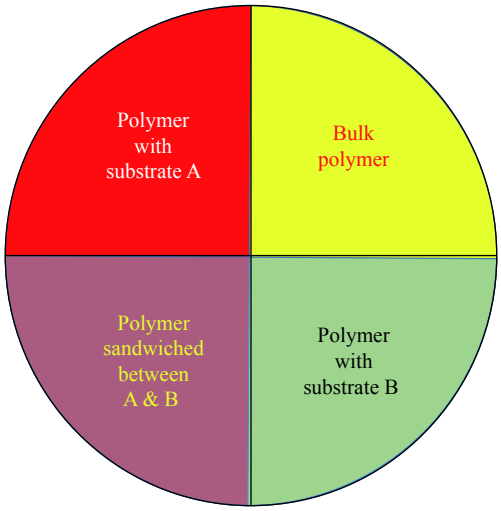

Fig. 1 A sketch depicting a sample with the testing polymer in contact with varied substrates in the same optical microscope view field

In the present work, the crystallization behavior of poly(ε-caprolactone) (PCL) system in bulk and at the surface of an oriented polyethylene (PE) or an oriented isotactic polypropylene (*i*PP) film was taken as an example system. Emphasis was given to a direct comparison of the nucleation ability of PE and *i*PP toward PCL under exactly the same experimental condition.

EXPERIMENTAL

Materials

Polyethylene (PE) used in this work was Lupolen 6021DX from BASF company, Germany. Isotactic polypropylene (*i*PP) was GB2401, with the melting flow index of 2.5 g/10min and the melting temperature of 170 °C, produced by Yanshan Petroleum and Chemical Company, China. Poly(ε-caprolactone) (PCL), with a weight-average molecular weight of 6.5×10^4 g·mol^{-1}, polydispersity of 1.53, and a melting temperature of 60 °C, was purchased from Aldrich Company.

Preparation

As presented in Fig. 2, the sample was prepared by first placing an oriented thin *i*PP film on a glass slide in the way that half of the glass slide has been covered by *i*PP (see part I), then transferring a thin PCL layer onto the surface of *i*PP and the glass slide uncovered with *i*PP (see part II), and finally depositing an oriented thin PE layer on the PCL surface in a way illustrated in part III. In this way, the sample was divided into four regions in the same view field under an optical microscope, which correspond to neat PCL (region 1), PCL/*i*PP (region 2), PE/PCL (region 3), and PE/PCL/*i*PP sandwich (region 4). Therefore, the crystallization behavior of PCL in bulk, at the surface of *i*PP or PE, and even sandwiched between *i*PP and PE could be compared directly during the melt-recrystallization of PCL under different conditions.

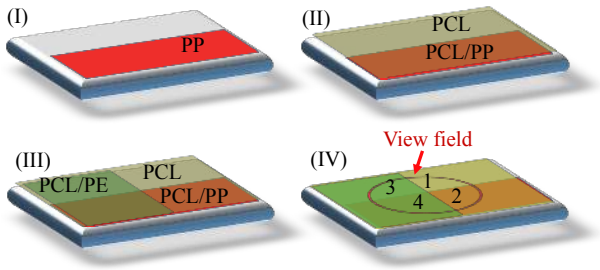

Fig. 2 A sketch showing the procedure of sample preparation

The used *i*PP and PE oriented thin films were prepared according to a melt-draw technique introduced by Petermann and Gohil[12] and Gohil *et al.*[13] According to this method, a small amount of a 0.5 wt% solution of PE or *i*PP in xylene was poured and spread uniformly on a preheated glass plate. The xylene solvent was allowed to evaporate at the preparation temperature of *ca*. 125 °C for PE and 140 °C for *i*PP, respectively. The remaining thin PE or *i*PP molten layer was then picked up by a motor-drive cylinder with a drawing speed of about 2 cm·s^{-1}. The thickness of the prepared film was around 50 nm, which was too thin to give any birefringence under optical microscope.

The used PCL thin film was prepared by dipping a clean glass slide into a 2 wt% PCL/chloroform solution. After the evaporation of chloroform, a PCL layer with the thickness of around 10 μm was then detached from the glass slide.

Characterization

The optical microimages were obtained by using the Axioskop 40A Pol optical microscope (Carl Zeiss) combined with a Linkam THMS600 temperature controller stage under crossed polarizers. For transmission electron microscopy (TEM) observation, a JEOL JEM-2100 TEM operated at 200 kV was used in this study. Phase contrast bright-field (BF) electron micrographs were obtained by defocus of the objective lens. In order to minimize the radiation damage by electron beam, the focusing was carried out on an area; then the specimen film was transferred to an adjacent undamaged area for recording the images immediately. AFM was conducted on a ScanAsyst (Bruker Co. Ltd.) instrument with a Dimension FastScan operated at room temperature in air. Measurements in the tapping mode were performed with OTESPA cantilevers (resonance frequency ≈ 318−339 kHz, spring constant ≈ 12−103 N·m^{-1}, scan rate = 3.92 Hz). Differential scanning calorimetry (DSC) measurements were conducted on a Q-2000 TA Instrumental DSC equipment with the cooling rate of 1 °C·min^{-1}.

https://doi.org/10.1007/s10118-019-2226-z

RESULTS AND DISCUSSION

Morphology of Melt-drawn PE and *i*PP Oriented Thin Films

The morphology of melt-drawn oriented thin films of *i*PP and PE has been frequently described in different literature.[14–26] For a better view to readers, the phase contrast bright field (BF) electron micrographs and the related electron diffraction patterns (insets) of the used PE and *i*PP melt-drawn films are presented in Fig. 3. The BF images of both PE and *i*PP melt-drawn thin films showed highly oriented lamellar structure, indicating the high degree of orientation. This was further confirmed by the electron diffraction patterns with sharp and well-defined reflection spots. It should be noted that a series of (*hk*0) diffraction spots appeared in the meridian direction for both PE and *i*PP, for instance, the (110), (200), and (020) for PE as well as the (110), (040), (130), and (060) for *i*PP. This demonstrated the fiber orientation of the melt-drawn PE and *i*PP thin films, that is to say, a sort of uniaxial orientation with the molecular chain direction (*i.e.*, the crystallographic *c*-axis) along with the drawing direction whereas the *a*- and *b*-axes rotating randomly about the *c*-axis.[27]

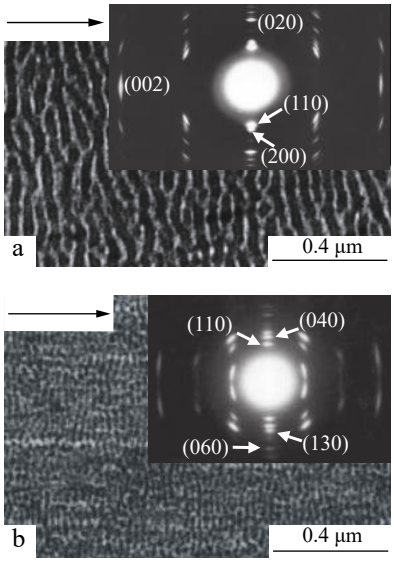

Fig. 3 Phase contrast BF electron micrographs and related electron diffraction patterns (insets) of highly oriented melt-drawn (a) PE and (b) *i*PP thin films. The arrows in the images indicate drawing direction of the films.

Morphology of PCL Crystallized at the Surfaces of Oriented PE and *i*PP Thin Films

Fig. 4 shows the AFM phase images of PCL crystallized at the surfaces of oriented PE and *i*PP thin films. From Fig. 4(a), it can be seen that the parallel-aligned edge-on lamellae of PCL were aligned perpendicularly to the molecular chain direction of PE, confirming the occurrence of parallel chain epitaxy of PCL on PE substrate. On the other hand, the crystallization of PCL on *i*PP substrate led to the formation of a cross-hatched lamellar structure with PCL edge-on lamellae oriented in the direction ±40° apart from the chain direction of *i*PP. In other words, PCL and *i*PP

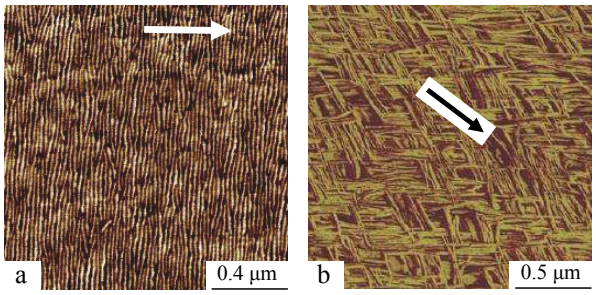

Fig. 4 Phase images of PCL crystallized on highly oriented melt-drawn (a) PE and (b) *i*PP thin films. The arrows in the pictures indicate molecular directions of the PE and *i*PP films, respectively. The thermal history of the samples were heat-treated at 80 °C for 10 min and then cooled naturally down to room temperature.

chains were ±50° apart from each other. These results indicated that both PE and *i*PP exhibited strong nucleation ability toward PCL and could initiate epitaxial crystallization of PCL, even though they had different orientations. They were in good agreement with the early literature report,[28–32] and therefore were not the scope of this work. We here focus mainly on the comparison of nucleation efficiency of PE and *i*PP toward PCL.

Comparison on the Nucleation Efficiency of PE and *i*PP Toward PCL

As mentioned in the introduction part, a nucleation efficiency parameter based on the peak crystallization temperatures of a polymer in bulk, with nucleation agent, and by self-seeding has been established to characterize quantitatively the nucleation efficiency of a nucleation agent on the polymer. Therefore, the crystallization DSC curves of PCL in bulk or at the surfaces of PE and *i*PP films are compared initially. As can be seen in Fig. 5, the peak crystallization temperature of PCL in bulk with the cooling rate of 1 °C·min^{-1} was estimated as 38.5 °C. *i*PP and PE have evidently enhanced the peak crystallization temperature of PCL. While the peak crystallization temperature of PCL at the *i*PP surface was elevated to 40.5 °C, PE led to the crystallization of PCL at peak temperature of 42.4 °C. These results clearly demonstrated the nucleation ability of *i*PP and PE on PCL. The nucleation efficiencies of *i*PP and PE toward PCL were, however, different. We recalled the nucleation efficiency

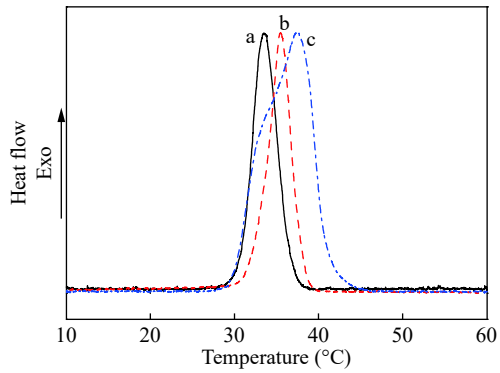

Fig. 5 DSC curves of PCL in (a) bulk, or at the surfaces of (b) *i*PP and (c) PE oriented thin films taken during the cooling from 80 °C down to 25 °C at a rate of 1 °C·min^{-1}

https://doi.org/10.1007/s10118-019-2226-z

parameter 100 × (T_{ca} − T_{c1})/(T_{c2} − T_{c1}). In the present case, the difference between the peak crystallization temperatures of PCL/*i*PP and PCL is 2, while that between PCL/PE and PCL is 3.9. This means that the nucleation efficiency of PE toward PCL was about 2 times greater than that of *i*PP. Besides, if the onset crystallization temperatures (T_{onset}) are considered, the results were then quite different. T_{onset}s of PCL in bulk, at the surfaces of *i*PP, and PE were approximately 44.5, 45.6, and 51.7 °C, respectively. When using T_{onset}s instead of T_{ca}s, the nucleation efficiency of PE toward PCL was then *ca*. 6.5 times higher than that of *i*PP.

From the above DSC results, a higher nucleation efficiency of PE than that of *i*PP toward PCL was unambiguously identified. This could be originated from either an early incidence of nucleation or an increased nucleation density, and the nucleation density depended on the active nucleation sites. In the present case, epitaxial crystallization of PCL took place on both *i*PP and PE substrates. Epitaxial crystallization is generally believed to occur when some lattice matchings are fulfilled between the substrate and the overgrowth polymer.[33–35] The crystal structure of PCL has been well studied.[36–39] It is generally accepted that the PCL chains with all-*trans* conformation pack in an orthorhombic unit cell with parameters of a = 0.748 nm, b = 0.498 nm, and c = 1.726 nm.[36] The PE planar zig-zag chains also pack in an orthorhombic unit cell but with parameters of a = 0.74 nm, b = 0.493 nm, and c = 0.2534 nm.[37,40] The almost identical unit cell parameters of PCL and PE along both *a*- and *b*-axes led to the existence of excellent matching between the interplane distance of every (*hk*0) lattice plane. For example, the mismatching between (100) and (010) lattice planes of them is only 1%. This implies that all of the PE lattice planes were active in nucleating PCL for epitaxial crystallization. On the other hand, the epitaxial crystallization of PCL on *i*PP has been explained in terms of the alignment of PCL zig-zag chain segments in the (100) lattice plane (d = 0.498 nm) along the methyl group rows in the (010) lattice plane of *α*-*i*PP (d = 0.505 nm) with a chain-row matching (mismatching is *ca*. 1.4%).[29,35] This means that only the (010) lattice planes of *α*-*i*PP can serve as active nucleation sites for PCL. We recalled that the melt-drawn PE and *i*PP films exhibited only a uniaxial orientation with molecular chains aligned in the same direction while the *a*- and *b*-axes rotated randomly about the *c*-axis. Taking this into account, the nucleation of PCL on melt-drawn *i*PP films could only happen at places where (010) lattice planes were exposed, whereas the nucleation of PCL on melt-drawn PE films occured at any exposed lattice planes. Therefore, much higher nucleation density of PCL on PE substrate than on *i*PP substrate was expected. In this case, when the sensitivity of DSC instrument was considered, the crystallization of PCL on PE would be certainly detected earlier than that on *i*PP substrate. If this is true, then the DSC result could not reflect the nucleation ability of *i*PP and PE toward PCL exactly. To avoid the possible misleading result, we observed directly the whole crystallization process of PCL in bulk as well as at the surfaces of *i*PP and PE substrates simultaneously.

Fig. 6 shows a series of optical micrographs of PCL taken during cooling at a rate of 1 °C·min^{-1}. With the help of experimental setup shown in Fig. 1, the crystallization of PCL in bulk as well as at the surfaces of *i*PP and PE substrates has been revealed simultaneously in the same view field. To eliminate the previous thermal history of PCL sample, the sample was first heated up to 80 °C for 10 min and then cooled at a rate of 1 °C·min^{-1} to room temperature. As presented in Fig. 6(a), the sample shows no birefringence at

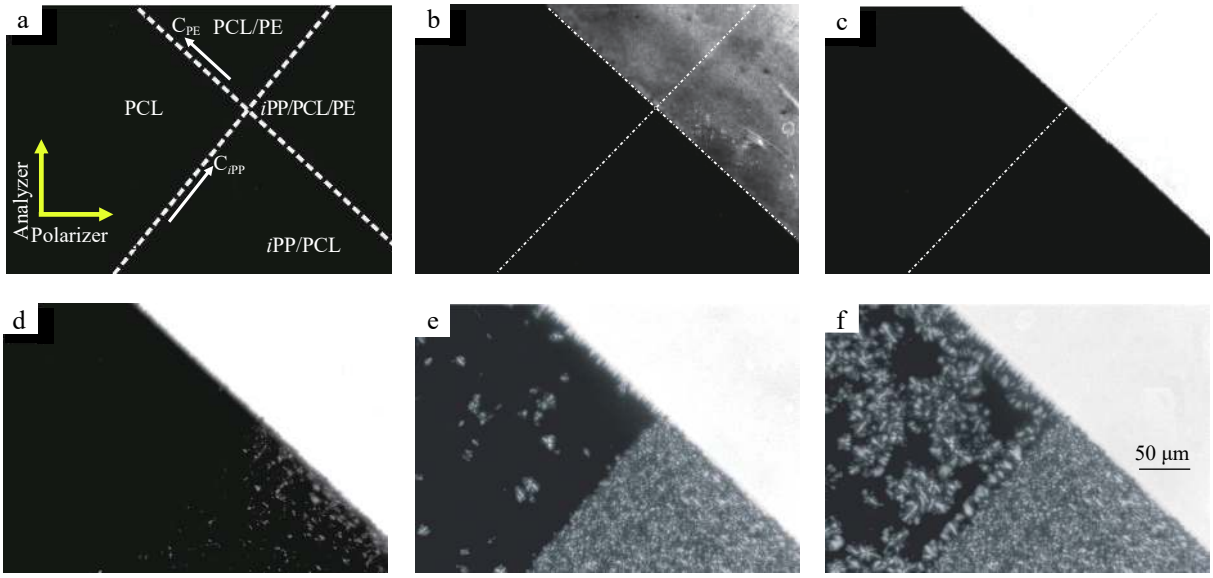

Fig. 6 Optical micrographs of PCL in bulk and at the surfaces of *i*PP and PE substrate films taken during the cooling process. The sample was first heated up to 80 °C for 10 min and then cooled at a rate of 1 °C·min^{-1} down to room temperature. The images were recorded at temperatures of (a) 80 °C, (b) 46 °C, (c) 44 °C, (d) 41 °C, (e) 39 °C, and (f) 37 °C. The dashed white lines trace out the boundaries of PE and *i*PP substrates, which have divided the sample into four regions as indicated. The white arrows labelled with PE and *i*PP indicate the molecular chain directions of PE and *i*PP, respectively. The yellow arrows with "polarizer" and "analyzer" describe the crossed polarization directions.

https://doi.org/10.1007/s10118-019-2226-z

80 °C, indicating that the PCL was in amorphous molten state and the *i*PP and PE substrates were too thin to show birefringence. For clarity, the boundaries of *i*PP and PE substrate films are indicated by the dashed white lines. From Fig. 6(b), it can be seen that weak birefringence appears fist in the PCL/PE and *i*PP/PCL/PE regions. The birefringence in these regions became stronger and stronger with further cooling the sample and reached the maximum at *ca*. 44 °C (Fig. 6c), reflecting the complete crystallization of PCL. The crystallization of PCL in bulk and *i*PP/PCL regions, however, did not take place at 44 °C. This meant that PE was more active in initiating the crystallization of PCL and the crystallization of PCL in both PCL/PE and *i*PP/PCL/PE regions was triggered by PE. When the temperature reached 41 °C (Fig. 6d), the crystallization of PCL in the *i*PP/PCL region has been initiated, while the crystallization of PCL in bulk did not occur at all. This indicated that *i*PP also exhibited nucleation ability toward PCL even though less pronounced as the PE. The crystallization of PCL at *i*PP surface finished at around 39 °C (Fig. 6e) and meanwhile the crystallization of PCL in bulk started. The crystallization of bulk PCL did not complete even when the sample was cooled to 37 °C (Fig. 6f). Fig. 7 shows the optical micrographs of the same sample as in Fig. 6 after cooled down to room temperature. It can be seen from Fig. 7(a) that the crystallization of PCL in all the regions was completed at that temperature. Due to the parallel alignment of PCL lamellae on the PE substrate through parallel chain epitaxy, light extinction in the area with PE substrate occured when the sample was rotated around the light beam axis for 45°, as seen in Fig. 7(b). The fully light extinction in the regions with PE, *e.g.* the PCL/PE and *i*PP/PCL/PE regions, indicated again that PCL crystallized on the PE side in the *i*PP/PCL/PE region.

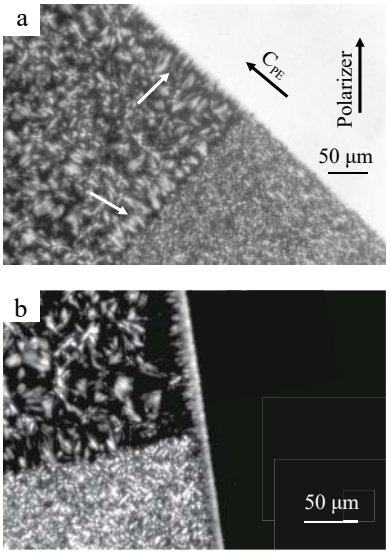

Fig. 7 Optical micrographs of PCL in bulk and at the surfaces of *i*PP and PE substrate films taken after cooling the sample from 80 °C down to room temperature. Part (b) is taken in the same area with part (a) but rotates 45° around the light beam axis. The white arrows in part (a) indicate the transcrystallization of PCL at the boundary of both PE and *i*PP. The black arrow labelled with PE indicates the molecular chain direction of oriented PE substrate.

According to the above experimental results, several aspects will be discussed in this section. First, in the cooling process at a rate of 1 °C·min^{-1}, the crystallization of PCL in contact with PE substrate started at a temperature above 46 °C while PCL in the PCL/*i*PP region started at a temperature near 41 °C. This was principally in agreement with the DSC results when possible time lag between visible birefringence and detectable exothermal is considered. Second, from Fig. 6, the crystallization of PCL at the PE and *i*PP surfaces completed at around 44 and 39 °C, respectively. Therefore, the difference between ($T_{ca} - T_{c1}$) for PCL/PE and PCL/*i*PP systems was about 5. It implied that the nucleation efficiency of PE toward PCL was 5 times higher than that of *i*PP when cooling at a rate of 1 °C·min^{-1}. Third, except for an early beginning of PCL crystallization at PE surface than that at *i*PP surface, the crystallization process of PCL at PE surface was completely different from those in bulk and at *i*PP surface. The crystallization of PCL on *i*PP surface was similar to the normal bulk crystallization process including nucleation and crystal growth. However, the nucleation of PCL on *i*PP took place earlier and the greater nucleation ability of *i*PP toward PCL enhanced the nucleation density of PCL compared with its bulk crystallization. The nucleation ability of *i*PP toward PCL has been well reflected by the appearance of transcrystalline zone at the boundary areas of PCL bulk and *i*PP/PCL regions as indicated by a white arrow. Consequently, microcrystallites with unique orientation due to epitaxy instead of spherulites were observed. On the contrary, the crystallization of PCL on PE substrate as a film developing process with weak birefringence first appeared at everywhere and then became stronger and stronger. This demonstrated that the active nucleation site of PCL on PE was indeed much higher than that on *i*PP. It is understandable since excellent matching fulfils between interplane distances of every (*hk*0) lattice plane of PCL and PE. In other words, the matching between both polymers is indeed very important for the heterogeneous nucleation between polymers. Fourth, except for the more active nucleation sites of PE toward PCL than that of *i*PP, which resulted in a much higher nucleation density of PCL on PE than on *i*PP, the nucleation of PCL occured also much earlier on PE than that on *i*PP. The greater nucleation ability of PE toward PCL than that of *i*PP has also evidently been reflected by the appearance of transcrystalline zone at the boundary area between the PCL/PE/*i*PP and PCL/*i*PP regions (see Fig. 7b). This might again demonstrate the importance of matching in initiating the epitaxial crystallization since the mismatching between PCL and *i*PP was somewhat larger than that between PCL and PE (1.4% versus 1%). Fifth, it should be noted that the above-mentioned crystallization behavior of PCL in different regions was reproducible during re-melting and recrystallization. Upon heating the sample as shown in Fig. 7 again up to 80 °C, PCL crystals in all the areas melted and the whole view field became dark again due to the disappearance of birefringence. During the cooling process, PCL melt-recrystallized almost in exactly the same way as described above. Therefore, such a method to compare the nucleating ability had a good reproducibility and provided reli-

able results. Moreover, the developed method for characterizing the nucleating ability of different substrates toward a polymer was an improvement over the mere use of nucleation densities.

CONCLUSIONS

A new method for characterizing the nucleating ability of different substrates toward a polymer under exactly the same thermal conditions has been presented in this study. It was based on the simultaneous optical microscopy observation of the polymer in bulk as well as at different substrates in the same view field. The developed method has been used to check the nucleation ability of PE and *i*PP toward PCL. Through *in situ* observation of PCL crystallization during cooling from 80 °C to room temperature in bulk as well as at the PE and *i*PP surfaces, conclusions can be drawn as follows.

(i) Both PE and *i*PP exhibited heterogeneous nucleation ability toward PCL, resulting in the epitaxial crystallization of PCL on PE and *i*PP. However, the nucleation ability of PE toward PCL was higher than that of *i*PP.

(ii) The higher nucleation ability of PE toward PCL was related to more active nucleation sites since the matching between the interplane distances of PE and PCL could be realized for every (*hk*0) lattice plane of both polymers owing to the identical unit cell parameters of them along *a*- and *b*-axes. On the contrary, a chain-row matching fulfiled only between the interchain distance of PCL in (100) lattice plane and the interrow distance of the out-sticking methyl groups in the (010) lattice plane of *α*-*i*PP. Taking the uniaxial orientation of both used PE and *i*PP substrate films into account, the nucleation of PCL on *i*PP substrate could take place only at places where the (010) lattice planes of *α*-*i*PP were exposed. As a result, less active nucleation sites for PCL existed on the uniaxially oriented *i*PP substrate. The difference in active nucleation sites resulted in different crystallization behavior of PCL on PE and *i*PP substrates. While a film developing process was observed for PCL crystallized on PE, PCL crystallized on *i*PP substrate through a traditional nucleation and crystal growth process, even though with higher nucleation density compared with that of its bulk crystallization.

(iii) Except for a higher nucleation density of PCL on PE than that on *i*PP, the nucleation of PCL took place much earlier on PE than that on *i*PP. This might imply that the matching condition was also important for initiating the epitaxial crystallization since the mismatching between PCL and *i*PP was somewhat larger than that between PCL and PE.

(iv) The reported results in this work were reproducible during repeated melting and recrystallization processes. This meant that the results produced by the used method were reliable, which was an improvement over the mere use of nucleation densities.

REFERENCES

1 Xu, J.; Zhang, Z.; Xu, H.; Chen, J.; Ran, R.; Li, Z. Highly enhanced crystallization kinetics of poly(L-lactic acid) by poly(ethylene glycol) grafted graphene oxide simultaneously as heterogeneous nucleation agent and chain mobility promoter. *Macromolecules* **2015**, *48*, 4891−4900.

2 Zhong, G.; Li, Z.; Li, L.; Shen, K. Crystallization of oriented isotactic polypropylene (*i*PP) in the presence of *in situ* poly(ethylene terephthalate) (PET) microfibrils. *Polymer* **2008**, *49*, 4271−4278.

3 Chen, L.; Zhou, W.; Su, F.; Zhang, W.; Chen, P.; Ji, Y.; Li, L. Filler-induced heterogeneous distribution of stretch-induced crystallization in natural rubber: An *in-situ* synchrotron-radiation micro-focused scanning X-ray diffraction study. *Polymer* **2017**, *115*, 217−223.

4 Kar, G. P.; Bose, S. Nucleation barrier, growth kinetics in ternary polymer blend filled with preferentially distributed carbon nanotubes. *Polymer* **2017**, *128*, 229−241.

5 Deng, H.; Xie, N.; Li, W.; Qiu, F.; Shi, A. C. Perfectly ordered patterns *via* corner-induced heterogeneous nucleation of self-assembling block copolymers confined in hexagonal potential wells. *Macromolecules* **2015**, *48*, 4174−4182.

6 Flieger, A. K.; Schulz, M.; Thurn-Albrecht, T. Interface-induced crystallization of polycaprolactone on graphite *via* first-order prewetting of the crystalline phase. *Macromolecules* **2018**, *51*, 189−194.

7 Chatterjee, A. M.; Price, F. P.; Newmann, S. Heterogeneous nucleation of crystallization of high polymers from the melt. I. Substrate-induced morphologies. *J. Polym. Sci., Part B: Polym. Phys.* **1975**, *13*, 2369−2383.

8 Chatterjee, A. M.; Price, F. P.; Newmann, S. Heterogeneous nucleation of crystallization of high polymers from the melt. II. Aspects of transcrystallinity and nucleation density. *J. Polym. Sci., Part B: Polym. Phys.* **1975**, *13*, 2385−2390.

9 Chatterjee, A. M.; Price, F. P.; Newmann, S. Heterogeneous nucleation of crystallization of high polymers from the melt. III. Nucleation kinetics and interfacial energies. *J. Polym. Sci., Part B: Polym. Phys.* **1975**, *13*, 2391−2400.

10 Fillon, B.; Lotz, B.; Thierry, A.; Wittmann, J. C. Self-nucleation and enhanced nucleation of polymers. Definition of a convenient calorimetric "efficiency scale" and evaluation of nucleating additives in isotactic polypropylene (*α* phase). *J. Polym. Sci., Part B: Polym. Phys.* **1993**, *31*, 1395−1405.

11 Fillon, B.; Wittmann, J. C.; Lotz, B.; Thierry, A. Self-nucleation and enhanced nucleation of polymers. Definition of a convenient calorimetric "efficiency scale" and evaluation of nucleating additives in isotactic polypropylene (*α* phase). *J. Polym. Sci., Part B: Polym. Phys.* **1993**, *31*, 1383−1393.

12 Petermann, J.; Gohil, R. M. A new method for the preparation of high modulus thermoplastic films. *J. Mater. Sci.* **1979**, *14*, 2260−2264.

13 Gohil, R. M.; Miles, M. J.; Petermann, J. On the molecular mechanism of the crystal transformation (tetragonai-hexagonai) in polybutene-1. *J. Macromol. Sci.-Phys.* **1982**, *B21*, 189−201.

14 Guan, G.; Zhang, J.; Sun, Li, H.; Yan, S.; Lotz, B. Oriented overgrowths of poly(L-lactide) on oriented isotactic polypropylene: A sequence of soft and hard epitaxies. *Macromol. Rapid Commun.* **2018**, *39*, 1800353.

15 Guo, Z.; Li, S.; Liu, X.; Zhang, J.; Li, H.; Sun, X.; Ren, Z.; Yan, S. Epitaxial crystallization of isotactic poly(methyl methacrylate) from different states on highly oriented polyethylene thin film. *J. Phys. Chem. B* **2018**, *122*, 9425−9433.

16 Ma, L.; Zhou, Z.; Zhang, J.; Sun, X.; Li, H.; Zhang, J.; Yan, S. Temperature-dependent recrystallization morphologies of carbon-coated isotactic polypropylene highly oriented thin films.

Macromolecules **2017**, *50*, 3582−3589.
17 Zhang, J.; Ruan, J.; Yan, S. Epitaxy of PLLA/PCL blends on highly oriented polyethylene substrate. *Acta Polymerica Sinica* (in Chinese) **2017**, 1524−1529.
18 Ma, L.; Zhang, J.; Memon, M. A.; Sun, X; Li, H; Yan, S. Melt recrystallization behavior of carbon coated melt-drawn oriented isotactic polypropylene thin films. *Polym. Chem.* **2015**, *6*, 7524−7532.
19 Zhou, H.; Yan, S. Can the structures of semicrystalline polymers be controlled using interfacial crystallographic interactions? *Macromol. Chem. Phys.* **2013**, *214*, 639−653.
20 Wu, J.; Zhou, H.; Liu, Q.; Yan, S. Application of electron diffraction in the structure characterization of polymer crystals. *Chinese J. Polym. Sci.* **2013**, *31*, 841−852.
21 Yan, C.; Guo, L.; Chang, H.; Yan, S. Induced crystallization of poly(ethylene adipate) by highly oriented polyethylene. *Chinese J. Polym. Sci.* **2013**, *31*, 1173−1182.
22 Li, H.; Yan, S. Surface-induced polymer crystallization and the resultant structures and morphologies. *Macromolecules* **2011**, *44*, 417−428.
23 An, Y.; Jiang, S.; Yan, S.; Sun J. R.; Chen, X. Crystallization behavior of polylactide on highly oriented polyethylene thin films. *Chinese J. Polym. Sci.* **2011**, *29*, 513−519.
24 Chang, H.; Guo, Q.; Shen, D.; Li, L.; Qiu, Z.; Wang, F.; Yan, S. A study on the oriented recrystallization of carbon-coated pre-oriented ultrathin polyethylene films. *J. Phys. Chem. B* **2010**, *114*, 13104−13109.
25 Yan, S. Origin of oriented recrystallization of carbon coated pre-oriented ultra-thin polymer films. *Macromolecules* **2003**, *36*, 339−345.
26 Yan, S.; Petermann, J.; Yang, D. Effects of lamellar thicknesses on the epitaxial crystallization of HDPE on the *i*PP substrate films. *Polym. Bull.* **1997**, *38*, 87−94.
27 Yang, D. C.; Thomas, E. L. An electron microscopy and X-ray diffraction study of the microstructures of melt-drawn polyethylene films. *J. Mater. Sci.* **1984**, *19*, 2098−2110.
28 Bu, X.; Li, H.; Yan, S. The propagation of crystal orientation in poly(ε-caprolactone)/poly(vinyl chloride) blend film after removal of induction layer. *Colloid Polym. Sci.* **2017**, *295*, 1635−1642.
29 Tao, X.; Yan, S.; Yang D. Epitaxial crystallization of poly(ε-caprolactone) on highly oriented isotactic polypropylene. *Chinese Chem. Lett.* **1993**, *4*, 1093−1096.
30 Liu, J.; Li, H.; Yan, S.; Xiao, Q.; Petermann, J. Epitaxial- and trans-crystallization of PCL on the highly oriented PE substrates. *Colloid Polym. Sci.* **2003**, *281*, 601−607.
31 Chang, H.; Zhang, J.; Li, L.; Wang, Z.; Yang, C.; Takahashi, I.; Ozaki, Y.; Yan, S. A study on the epitaxial ordering process of the polycarprolactone on the highly oriented polyethylene substrate. *Macromolecules* **2010**, *43*, 362−366.
32 Yan, C.; Li, H.; Zhang, J.; Ozaki, Y.; Shen, D.; Yan, D.; Shi, A. C.; Yan, S. Surface induced anisotropic chain ordering of polycarprolactone on oriented polyethylene substrate: Epitaxy and soft epitaxy. *Macromolecules* **2006**, *39*, 8041−8048.
33 Wittmann, J. C.; Lotz, B. Epitaxial crystallization of aliphatic polyesters on trioxane and various aromatic hydrocarbons. *J. Polym. Sci., Part B: Polym. Phys.* **1981**, *19*, 1853−1864.
34 Wittmann, J. C.; Lotz, B. Epitaxial crystallization of polyethylene on organic substrates: A reappraisal of the mode of action of selected nucleating agents. *J. Polym. Sci., Part B: Polym. Phys.* **1981**, *19*, 1837−1851.
35 Wittmann, J. C.; Lotz, B. Epitaxial crystallization of polymers on organic and polymeric substrate. *Prog. Polym. Sci.* **1990**, *15*, 909−948.
36 Hu, H.; Dorset, D. L. Crystal structure of poly(ε-caprolactone). *Macromolecules* **1990**, *23*, 4604−4607.
37 Bittiger, H.; Marchessault, R. H.; Niegisch, W. O. Crystal structure of poly-ε-caprolactone. *Acta Cryst.* **1970**, *B26*, 1923−1927.
38 Chatani, Y.; Okita, Y.; Tadokoro, H.; Yamashita, Y. Structural studies of polyesters. III. Crystal structure of poly-ε-caprolactone. *Polym. J.* **1970**, *1*, 555−562.
39 Núñeza, E.; Ferrandoa, C.; Malmströma, E.; Claessona, H.; Wernerb, P. E.; Gedde, U. W. Crystal structure, melting behaviour and equilibrium melting point of star polyesters with crystallisable poly(ε-caprolactone) arms. *Polymer* **2004**, *45*, 5251−5263.
40 Bunn, C. W. The crystal structure of long-chain normal paraffin hydrocarbons. The "shape" of the $>CH_2$ group. *Trans. Faraday Soc.* **1939**, *35*, 482−491.

https://doi.org/10.1007/s10118-019-2226-z